We are IntechOpen, the world's leading publisher of Open Access books Built by scientists, for scientists

4,800
Open access books available

122,000
International authors and editors

135M
Downloads

Our authors are among the

154
Countries delivered to

TOP 1%
most cited scientists

12.2%
Contributors from top 500 universities

CLARIVATE ANALYTICS BOOK CITATION INDEX INDEXED

WEB OF SCIENCE™

Selection of our books indexed in the Book Citation Index in Web of Science™ Core Collection (BKCI)

Interested in publishing with us?
Contact book.department@intechopen.com

Numbers displayed above are based on latest data collected.
For more information visit www.intechopen.com

6

Advanced Torque Control Scheme for the High Speed Switched Reluctance Motor

Dong-Hee Lee, So-Yeon Ahn and Jin-Woo Ahn
Dept. of Mechatronics Engineering, Kyungsung University
Republic of Korea

1. Introduction

High speed drive systems are much interested in the industrial application such as blower, compressor, pump and spindle due to the compact size and high efficiency. In recent, the demands of high speed drives are much increased due to the mechanical advantages of high speed system. SRMs (Switched Reluctance Motors) have simple structure and inherent mechanical strength without rotor winding and permanent magnet. These mechanical structures are suitable for harsh environments such as high temperature and high speed applications. Although SRMs have many advantages for the high speed applications, high torque ripple is still main problem to be applied to a high speed drives.

SRM(Switched Reluctance Motor) has been researched in last 150 years. However, significant amount of attention to this motor type was given in last few decades thank to the development of microcontrollers, power semiconductors and CAD technology. But compared with other motor, SRM cannot be operated without inverter. Therefore, it is suitable for variable speed application because inverter is essential.

SRM is a doubly salient machine because both the stator and rotor have salient poles. Flux is created by concentrated stator winding only. There are no permanent magnets, commutators, and windings in rotor side. So, SRM has simple and robust rotor structure that is very important in high speed application because centrifugal force is very high when rotor rotates at high speed. Due to a simple structure at the stator and the rotor, SRM can compete with other types of motor. And because SRM has only the windings at the stator, SRM achieves high efficiency especially in high speed region. With these advantageous features, SRM deserves to be investigated and it is good candidate for high speed drive systems in particular.

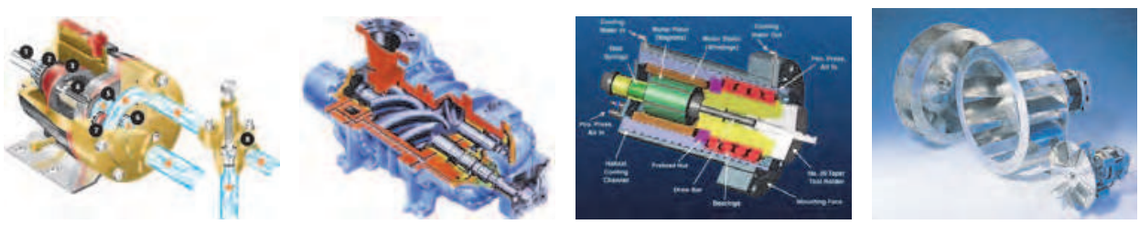

Fig. 1. Applications of a high speed drive.

2. Switched reluctance motor (SRM)

The SRM is an electric machine that converts the reluctance torque into mechanical power. In the SRM, both the stator and rotor have a structure of salient-pole, which contributes to produce a high output torque. The torque is produces by the alignment tendency of poles. The rotor will shift to a position where reluctance is to be minimized and thus the inductance of the excited winding is maximized. The SRM has a doubly salient structure, but there are no windings or permanent magnets on the rotor. The rotor is basically a piece of steel (and laminations) shaped to form salient poles. So it is the only motor type with salient poles in both the rotor and stator. As a result of its inherent simplicity, the SRM promises a reliable and a low-cost variable-speed drive and will undoubtedly take the place of many drives now using the cage induction, PM and DC machines in the short future. The number of poles on the SRM's stator is usually unequal to the number of the rotor to avoid the possibility of the rotor being in a state where it cannot produce initial torque, which occurs when all the rotor poles are aligned with the stator poles.

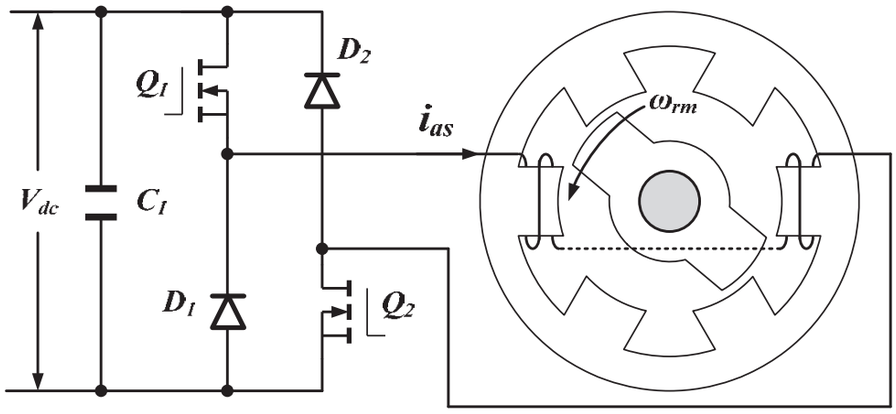

(a) General 6/2 SRM

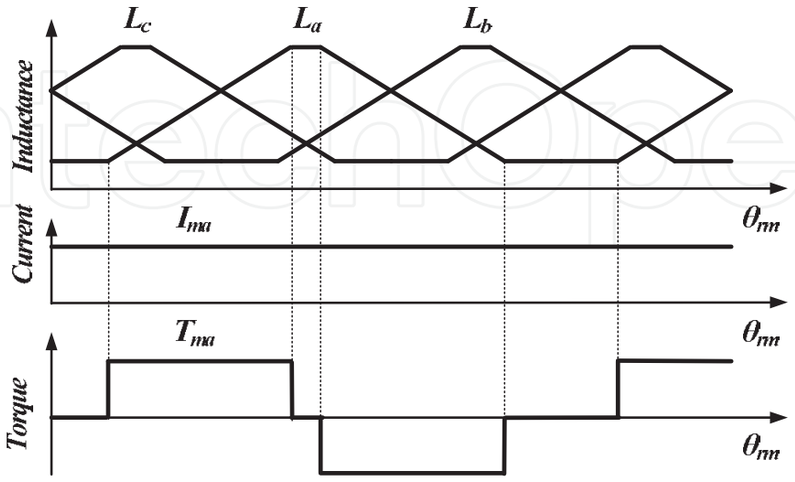

(b) Output torque vs phase current

Fig. 2. SRM drive system.

Fig. 2 shows a general SRM drive system. With a constant phase current, the ideal phase torque is produced according to the square of current and inductance slope of the motor. Two basic equations of an SRM can be derived in terms of phase voltage and torque as follows.

$$v = R \cdot i + L(\theta_{rm}, i) \cdot \frac{di}{dt} + i \cdot \frac{dL(\theta_{rm}, i)}{d\theta_{rm}} \cdot \omega_{rm} \tag{1}$$

$$T_m = \frac{1}{2} \cdot i^2 \cdot \frac{dL(\theta_{rm}, i)}{d\theta_{rm}}\Big|_{i=constant} \tag{2}$$

where, R: resistor of phase winding. θ_{rm} : rotor position, ω_{rm}: rotor speed, $L(\theta_{rm},i)$: inductance is linearly varying with rotor position for a given current. However, the torque characteristics of SRM can be improved by the rotor and stator design.
Fig. 3 shows the various type of 4/2 SRMs. The modified types which have a staggered gap rotor pole surface, air teeth and air hole types of rotor pole are introduced.

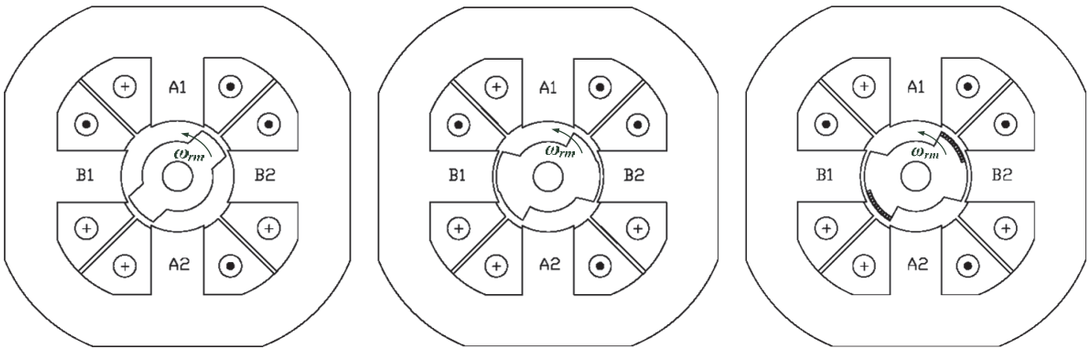

(a) Conventional type (b) Staggered gap type (c) Air teeth type

Fig. 3. Various type of 4/2 SRM.

Due to magnetic nonlinearity in an SRM, the phase inductance is nonlinear with respect to rotor position and phase current, and hence, constant torque profiling for torque ripple reduction is difficult compared to conventional AC motors such as PM and induction motors.

2.1 Mechanical structures

Constructions of SRM with no magnets or windings on the rotor also bring some disadvantage in SRM. Since there is only a single excitation source and but also magnetic saturation, the power density of reluctance motor is lower than PM motor. The construction of SRM is shown in Fig. 4. The dependence on magnetic saturation for torque production, coupled with the effects of fringing fields, and the classical fundamental square wave excitation result in nonlinear control characteristics for the reluctance motor. The double saliency construction and the discrete nature of torque production by the independent phases lead to higher torque ripple compared with other machines. The higher torque ripple, and the need to recover some energy from the magnetic flux, also cause the ripple current in the DC supply to be quite large, necessitating a large filter capacitor. The doubly salient structure of the SRM also causes higher acoustic noise compared with other

machines. The main source of acoustic noise could induce the radial magnetic. So higher torque ripple and acoustic noise are the most critical disadvantages of the SRM.

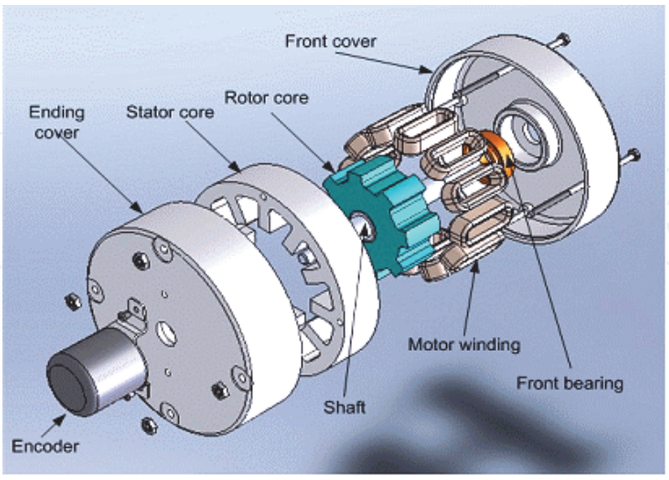

Fig. 4. The construction of SRM.

The absence of permanent magnets imposes the burden of excitation on the stator windings and converter, which increases the converter kVA requirement. Compared with PM brushless machines, the per unit stator copper losses will be higher, reducing the efficiency and torque per ampere. However, the maximum speed at constant power is not limited by the fixed magnet flux as in the PM machine, and hence, an extended constant power region of operation is possible in SRM.

2.2 Torque and torque ripple

The torque ripple of the SRM is divided to three parts. The first source is from the inherent torque ripple due to the mechanical and magnetic structure. Single-and two-phase SRMs have inherent torque dead-band due to an absence of the torque over-lap region between phases. Fig. 5 and Fig. 6 show the output torque according to the phase current in conventional single-and two-phase SRMs. As shown in Fig. 5 and 6, the positive torque region has dead-band from the inherent magnetic structure.

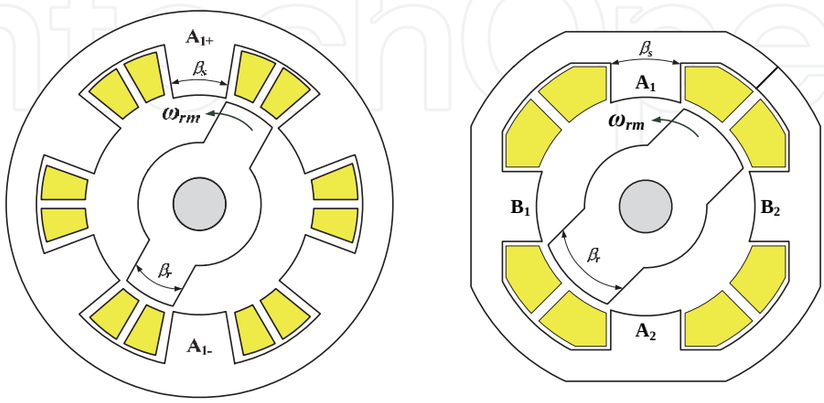

(a) Single phase SRM (b) Two-phase SRM

Fig. 5. Mechanical structure of single and two-phase SRMs.

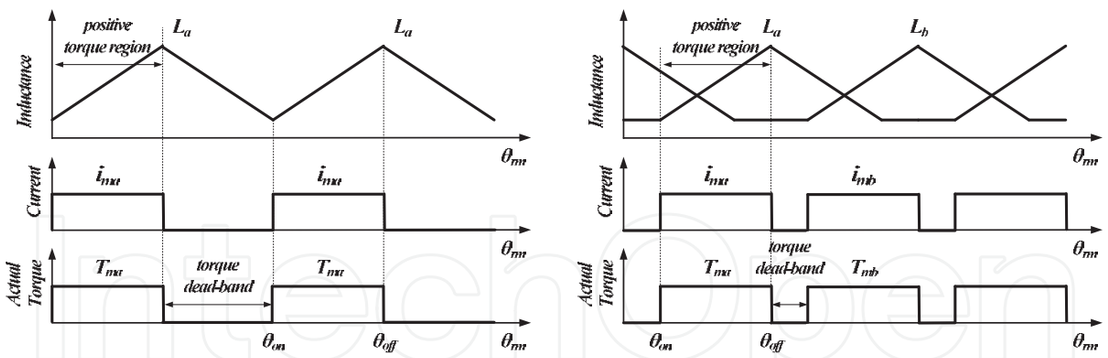

(a) Single phase SRM (b) Two-phase SRM

Fig. 6. Inductance, current and output torque of single and two-phase SRMs.

In order to overcome the inherent torque dead-band, asymmetric SRMs are investigated. These types have wide positive torque region with a short negative torque region, and are useful in an unidirectional application such as blowers and fans. For the single phase SRM, hybrid type using permanent magnet is researched. The inserted permanent magnet can produce cogging torque during torque dead-band. However, the torque of the inserted PM poles cannot be controlled, so it has high torque ripple but smaller than a conventional single-phase SRM. In two-phase SRM, rotor pole shapes can be changed to extend the torque region, and the inductance has asymmetric characteristics shown in Fig. 7.

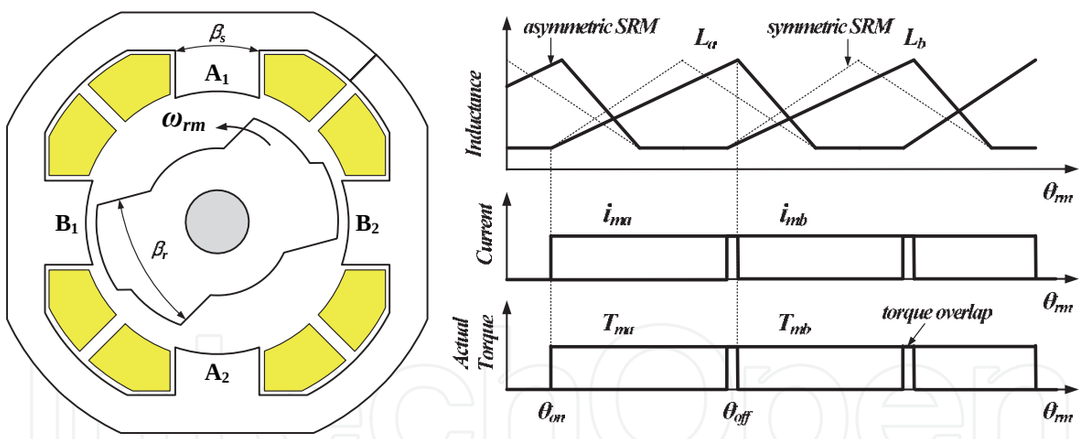

(a) Stepper rotor type SRM (b) Inductance, current and torque characteristics

Fig. 7. Uni-directional 4/2 SRM with torque overlap.

As shown in Fig. 7, the stepper rotor type has a wide rotor pole arc that produces torque overlap between two phases. In order to extend positive torque region, the inductance has asymmetric characteristics shown in Fig. 7(b), and is useful for an unidirectional application. It can remove torque dead-band, but torque ripple during stepper region is much serious. To reduce the torque ripple of stepper region, optimization design process can be adopted. From these research results, the inherent torque dead-band can be reduced.

The other is from the non-linear characteristics of inductance and un-constant torque by the constant current due to the saturation effect. Although the output torque is proportional to the inductance gradient, the inductance gradient is not constant. The inductance has non-

linear according to rotor position due to the saturation effect. So, the constant phase current cannot guarantee a constant torque shown as Fig. 8. In the compact size motor, flux saturation is essential. So, the output torque ripple is different according to the load condition.

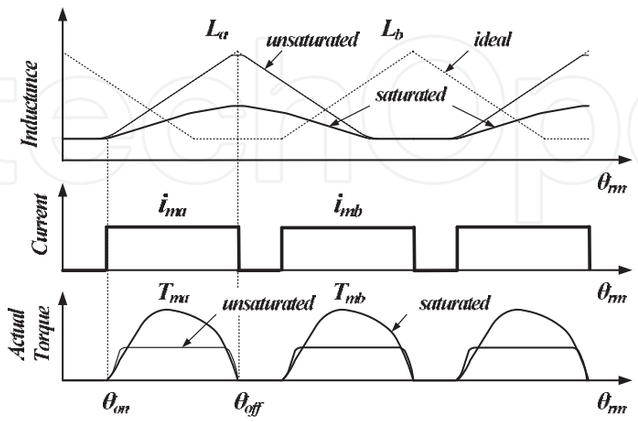

Fig. 8. Non-linear torque from the saturation effect.

In order to reduce the torque ripple from the saturation and non-linear characteristics, advance torque control scheme is required. In the next chapter, the detailed torque control schemes will be explained.

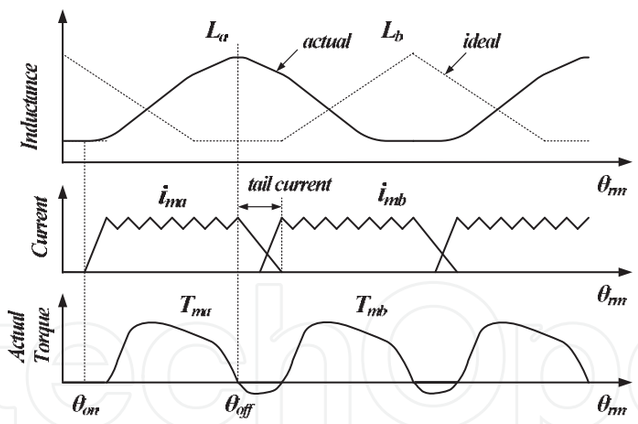

Fig. 9. Torque ripple from the tail current.

One reason of torque ripple is negative torque due to the tail current. The output torque of a phase is changed by the inductance slope. If the phase current is extended to the opposite torque region, the current produces the opposite torque. In the high speed or heavy load condition, the phase current is not extinguished in the same torque region, and the extended tail current produces negative torque as shown in Fig. 9. When the turn-off angle is controlled to remove the tail current, negative torque can be removed. However, the tail current is much serious in the high speed application due to a short commutation time. In order to reduce the negative torque effect, additional torque compensation algorithm and boost converter with a high negative demagnetization voltage have been researched. If the

turn-off angle is much advanced to reduce the tail current, the effective torque region is much decreased with low efficiency and low output torque. The boost converter which can supply the high excitation and demagnetization voltage can reduce the commutation time, and it is useful to remove the tail current.

3. Torque control schemes

Various torque control schemes are investigated for the efficiency and torque ripple reduction. The torque control of SRMs is classified by three categories : on/off angle control, current control and direct torque control. The on/off angle control and current control schemes are simple and don't use any torque estimation. For a better performance, current control scheme uses on/off angle changing according to the load condition. In these control schemes, they didn't consider non-linear characteristics. So, the output torque of SRM is dependent on the saturation effect and inductance characteristics.

Fig. 10, 11 and 12 show the phase current and output torque of on/off angle control, current control and current control with on/off angle controller. The on/off angle control scheme uses a single pulse voltage during turn-on and-off angle (dwell angle). As shown in Fig. 10(b), the output torque is controlled by average value during dwell angle , and PWM switching is not used. So, the switching loss is very small compared with the current control scheme, but the output torque has large ripple. In the Fig. 10(a), the torque of phase A is controlled by turn-on angle controller, and phase B is controlled by turn-off angle controller. When the turn-on angle is advanced ($\theta_{onA1} < \theta_{onA3}$), the phase current and output torque is changed according to the turned on region. Much increased phase current i_{ma1} can increase the output torque than the small phase current i_{ma3} . Similarly, when the turn-off angle is delayed ($\theta_{offB1} < \theta_{offB3}$), the phase current and output torque range is changed according to the turned off angle. Much extended phase current i_{mb3} can increase the output torque than the short phase current i_{mb1} . This control scheme just controls average torque, and cannot control the instantaneous torque.

Fig. 11 shows a current control block diagram, phase current and output torque. Hysteresis current controller or PWM(Pulse Width Modulation) can be used to adjust the phase current. In the current controller, the activated phase is determined by the rotor position. By the switching of power devices, the switching loss is much increased than the on/off angle control method. But, excitation current can be controlled with flat-top shape. If the output torque is linearly proportional to the phase current, a constant output torque can be obtained. However, the output torque of SRM has non-linear characteristics due to the inductance and saturation effect. So, the output torque is dependent on the non-linear torque characteristics.

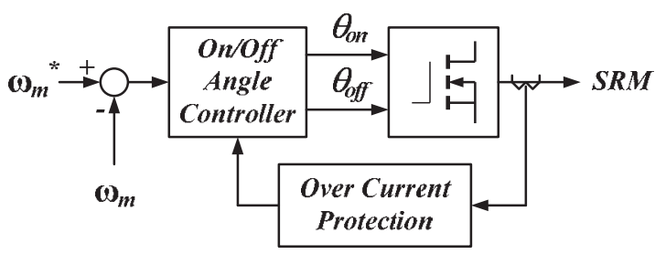

Fig. 10. (a) On/off angle controller.

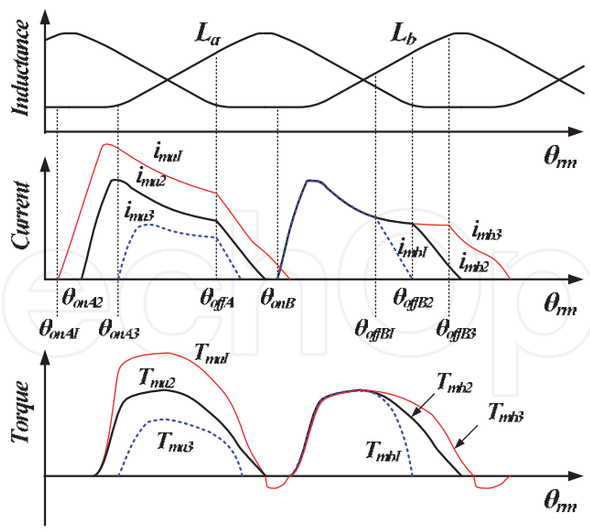

(b) Phase current and output torque.

Fig. 10. Phase current and output torque of the on/off angle control scheme.

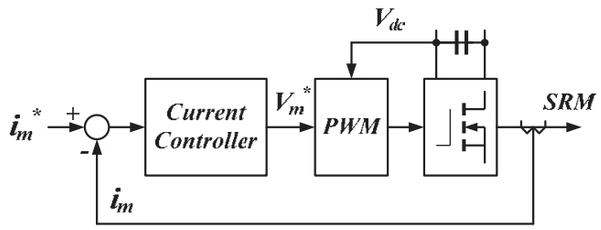

(a) Current control scheme

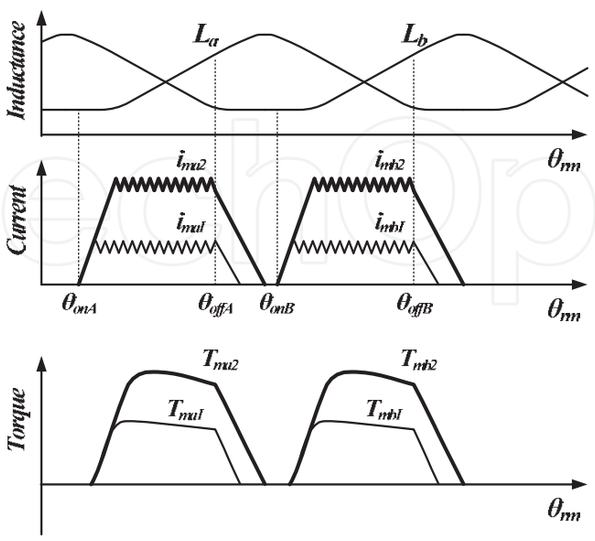

(b) Phase current and output torque

Fig. 11. Phase current and output torque of current control scheme.

In order to build up the desired current and extinguish the demagnetized current, turn-on and-off angles are very important. So, the current controller with angle adjusting can increase the torque performance. Although, the output torque is dependent on the non-linear characteristics, but the torque region can be adjusted according to the load condition. In a heavy load with high reference current, the turn-on angle is advanced to ensure the excitation current building-up time. On the contrary, the turn-off angle is delayed in the light load with low reference current due to the efficiency. Because the output torque cannot be produced during minimum inductance and maximum inductance region, the phase current of these region is much contributed to the loss.

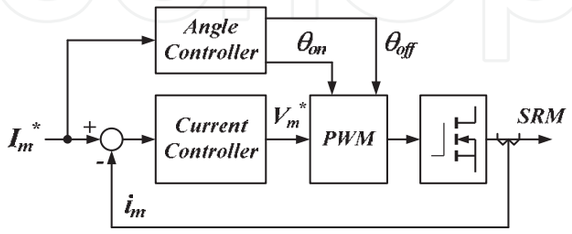

(a) Current control scheme with angle controller

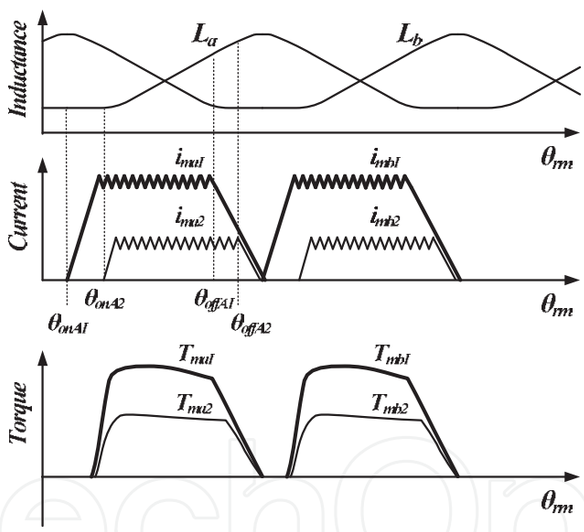

(b) Phase current and output torque

Fig. 12. Phase current and output torque of the current control with on/off angle controller

The other torque control methods are current shape, direct torque control and TSF(Torque Sharing Function) technologies. These torque control methods are complex but torque ripple can be reduced. In order to reduce the torque ripple, the non-linear characteristics are considered in these control schemes. To compensate the output torque variation according to the current and rotor position, motor characteristics are included in the controller by look-up table, data memory and simplified mathematical model.

The current shape control method uses a compensation current according to the rotor position to compensate the saturation effect. In this control method, the compensation term is calculated with a simplified model. So, the torque ripple is not perfectly rejected.

More advance torque control method uses a torque to current data to reduce the torque ripple. In this approach, the reference current is changed according to the rotor position and reference torque with the motor characteristics. The torque to current data is determined by the actual motor characteristics and has 3-dimensions. Fig. 13 shows the torque control scheme using torque-to-current data, and its operating characteristics consideration. As shown in Fig. 13(b), the reference current to produce the desired output torque is not constant, and non-linear current reference is determined by the torque-to-current data. The current controller is designed to keep the reference current. This approach needs a complex database to compensate the motor characteristics, but the torque ripple can be reduced. The output torque is dependent on the accuracy of the torque-to-current data and current controller. When the torque-to-current data is very accurate, the output torque is very constant during a single phase excitation. But, it has torque ripple during the commutation region.

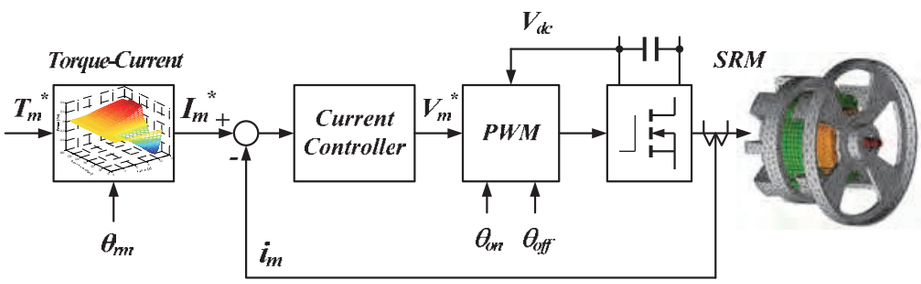

(a) Non-linear current control scheme

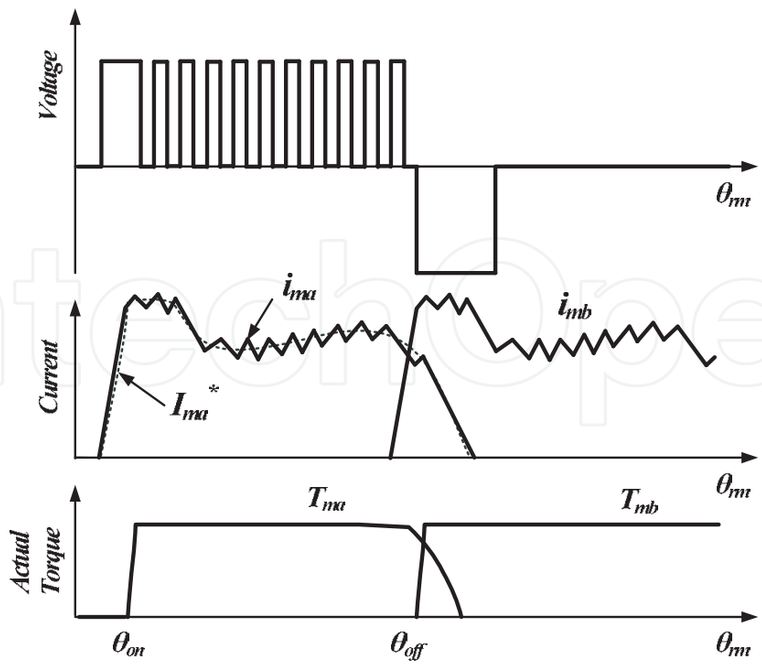

(b) Operating characteristics

Fig. 13. Non-linear current control scheme and its operating characteristics.

Another approach such as TSF uses a torque references and torque sharing during commutation region. In the TSF method, torque region is divided by two region : single-phase mode and two-phase mode. In a single-phase mode, only one phase current produces the output torque. In a two-phase mode, the outgoing phase and incoming phase current produce the output torque, and the total torque is the sum of the two phases. In order to reduce the torque ripple during the commutation region, torque references should be changed, and the sum of the torque references of the each phases are constant. The reference torque of the outgoing phase is decreased, and the reference torque of the incoming phase is increased during this region. The increasing and decreasing torque reference can be determined as linear and sinusoidal function. Fig. 14 shows a TSF method using sinusoidal function.
As shown in Fig. 14(b), torque reference of phase A is increased, and reached the target value between θ_{onA} and θ_{offB}, the reference of phase B is decreased from target value to zero, reversely. However, the sum of two-phase is same as target value. When the phase current can keep the reference current, the output torque of SRM can keep the constant value with a small torque ripple due to the current switching. Similar to the non-linear current control scheme, TSF needs a torque-to-current data to produce the reference current which generates a reference torque according to the rotor position. As we shown in previous control scheme, the output torque of the TSF method is dependent on the accuracy of the data and current control performance.

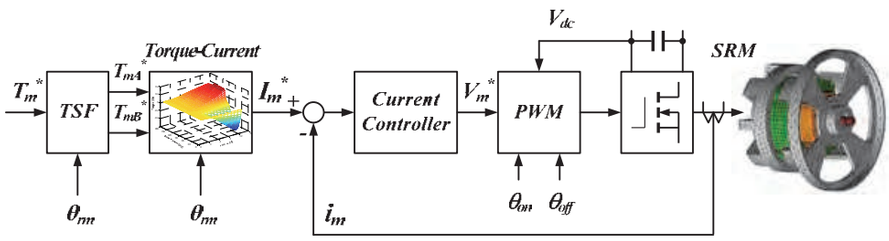

(a) TSF control scheme

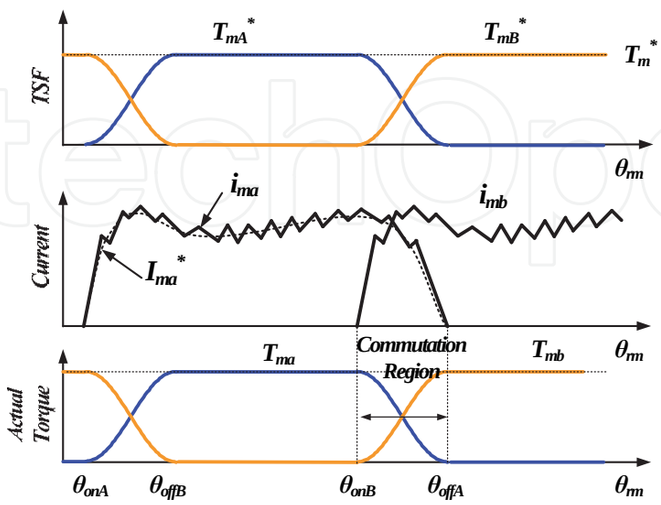

(b) Operating characteristics of the TSF control scheme

Fig. 14. TSF control scheme and its operating characteristics.

The torque reference during one-phase mode of the each phases is defined as follows.

$$f^*_{T(k)} = T^*_m$$
$$f^*_{T(k-1)} = 0 \tag{3}$$

And the torque commands during commutation are defined as follows in the cosine TSF.

$$f^*_{T(k)} = \left[1 - \cos\left(\frac{\theta_{rm} - \theta_{on(k)}}{\theta_{off(k-1)} - \theta_{on(k)}} \cdot \frac{\pi}{2}\right)\right] T^*_m \tag{4}$$
$$f^*_{T(k-1)} = 1 - f^*_{T(k)}$$

Where, θ_{rm} is rotor position. The $\theta_{on(k)}$ and $\theta_{off(k-1)}$ are turn-on and-off angles of the incoming and outgoing phases, respectively.

Compared with TSF method, DTC(Direct Torque Control) scheme uses a torque estimator and simple switching rules to control the output torque. The torque estimator is similarly made using the non-linear torque characteristics of the motor according to the phase current and rotor position. And these data reflect the saturation effect and the inductance characteristics. The DTC uses a direct torque comparison method with the torque estimator, the switching rules are designed to compensate the torque error between the torque reference and the estimated torque. The switching technologies of the DTC algorithm act as hysteresis controller. For the effective compensation of the torque error, the switching technologies can use PWM method.

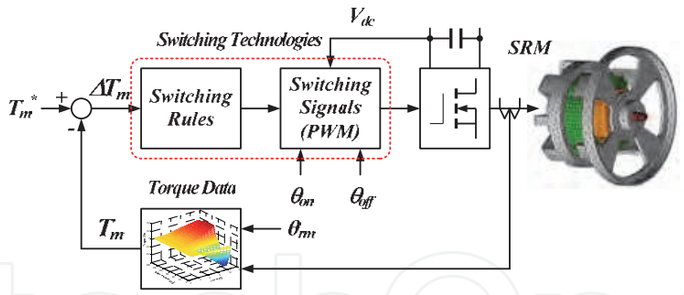

(a) Block diagram of the direct torque control scheme.

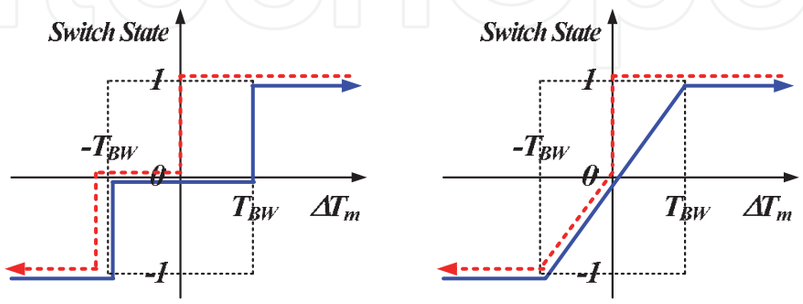

(b) Switching rule without PWM (c) Switching rule with PWM

Fig. 15. Direct torque control scheme.

Fig. 15 shows the DTC control block diagram and the examples of switching rules. The switching state of the switching rule means the operating modes of converter. And the T_{BW} is the torque error band of the DTC. The switching state 1 is excitation mode which supplies the dc-link voltage in the phase winding. The switching state 0 is free-wheeling mode which supplies zero voltage, and one power devices of the converter is turned on. And the switching state -1 is the demagnetization mode which supplies negative dc-link voltage in the phase winding. During the demagnetization mode, power devices of the phase winding are fully turned off. With the PWM technology, the switching state can move more smoothly. The PWM duty ratio is controlled by the torque error within the switching states. The PWM method can guarantee the fixed switching frequency with small torque ripple.

The previous researches are very useful to reduce the torque ripple of SRM in the conventional speed region. In the region, the main torque ripple is from the inherent torque dead-zone and non-linear torque characteristics. So, the DTC and TSF can reduce the torque ripple from the non-linear torque characteristics with the accurate torque data.

4. Advanced torque control scheme for a high speed SRM

4.1 Advanced converter topologies

When the motor speed is increased, the switching and excitation time are much decreased. The phase current of an AC machine has sinusoidal waveform, and current changing is very smooth. However, the phase current of SRM has square waveform. And the changing of the phase current is very rapid. Sometimes, the excitation current cannot be reached to the desired value, and the demagnetization cannot be extinguished during the commutation time due to a short excitation and demagnetization time in a high speed region. The insufficient excitation current makes an insufficient output torque, and the extended demagnetization can produce a negative torque. The much advanced turn-off angle can reduce the tail current in a high speed, but the output torque is not sufficient due to a short excitation region.

Fig. 16 shows the current and torque waveforms in a high speed region.

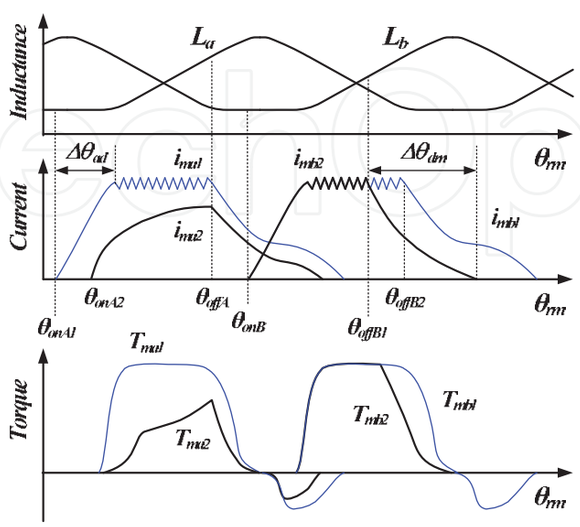

Fig. 16. Current and torque in a high speed.

As shown in Fig. 16, a short excitation and demagnetization time can produce a high torque ripple. Compared with i_{ma1} and i_{ma2}, the phase current i_{ma2} cannot be reach the desired value due to a short excitation time. So, the output torque has a high torque ripple. With the extended advance angle, the phase current can be reached to the desired value. Similarly, the turn-off angle should be advanced to reduce the tail current. In Fig. 16, the phase current i_{mb1} is extended to the negative torque region, and it produces a negative torque due to the tail current. With an advance turn-off angle, the phase current i_{mb2} is extinguished during the proper torque region, but the active torque region is decreased. The decreased active torque region from the advanced turn-off angle makes high torque ripple due to the torque dead-band.

Fig. 17 shows the phase current in the high speed region with an asymmetric converter. As shown in Fig. 17, the motor is excited at θ_{on} advanced $\Delta\theta_{ad}$ from the start point of positive torque region θ_{min} to establish sufficient torque current. The desired phase current is represented by dashed line in Fig. 17 and is demagnetized at θ_{off}, and decreased to zero before the starting point of the negative torque region θ_{max} so as not to develop negative torque.

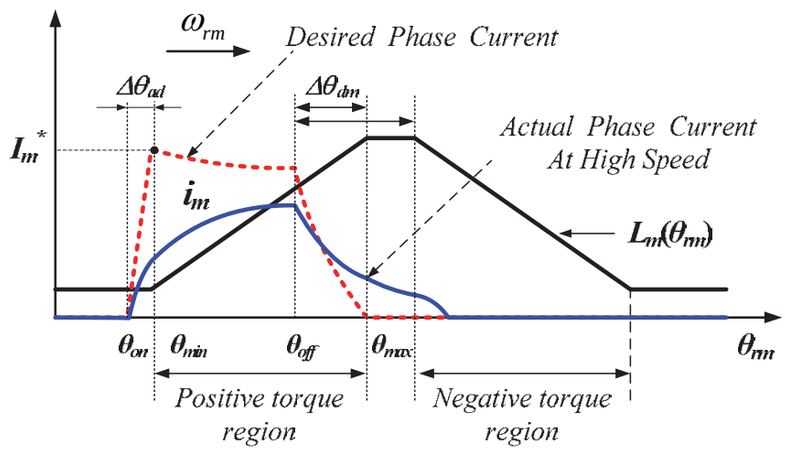

Fig. 17. Current in a high speed region.

In order to secure enough time to build-up the desired phase current I_m^*, the advance angle $\Delta\theta_{ad}$ can be adjusted according to motor speed ω_{rm}. From the voltage equations of the SRM, the proper advance angle can be calculated by the current rising time as follows regardless of phase resistance at the turn-on position

$$\Delta\theta_{ad} = L_{\min}\frac{I_m^*}{V_m} \tag{5}$$

$$\Delta\theta_{dm} = L_m(\theta_{off}, i_m)\frac{i_m}{V_m} \tag{6}$$

$$\Delta t_{ad} = \frac{\Delta\theta_{ad}}{\omega_{rm}} \tag{7}$$

$$\Delta t_{dm} = \frac{\Delta\theta_{dm}}{\omega_{rm}} \tag{8}$$

Where, I_m^* is the desired phase current, and V_m is the terminal voltage of the phase winding. As speed increases, the advance and demagnetization angles are increased and turn-of and turn-off positions may be advanced to the negative torque region of the previous phase.
If the actual terminal voltage is assumed as dc-link value, the actual maximum phase current can be obtained when the advance angle is in the previous unaligned position.

$$I_{\max} = \frac{\Delta\theta_{ad} \cdot V_{dc}}{L_{\min} \cdot \omega_{rm}} \tag{9}$$

And, the maximum output torque at θmin can be derived as follow.

$$T_{\max} = \frac{1}{2} \cdot I_{\max}^2 \frac{dL(\theta_{rm})}{d\theta_{rm}} \tag{10}$$

With a fixed turn-on position, the actual phase current which is denoted by a solid line cannot reach the desired value in the high speed region as shown in Fig. 17.
In a high speed, the advance and demagnetization time are much decreased. In order to reduce the torque ripple, the phase current should be well controlled. However, the short excitation and demagnetization times make a high current error in a high speed region.
In order to overcome these problems, boost voltage convertershas been researched. Fig. 18 shows the 4-level converter for high speed SRM.

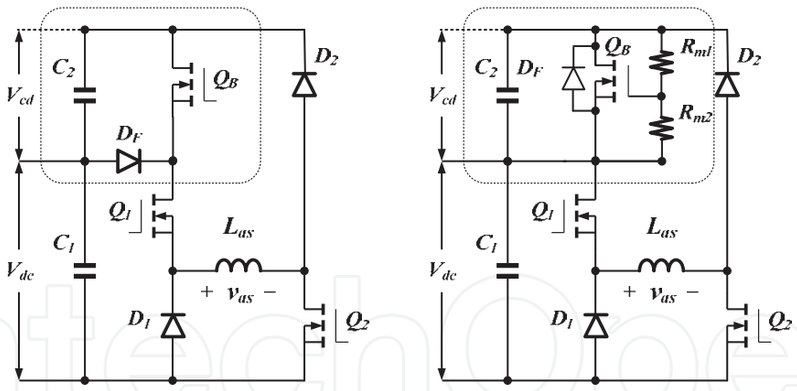

(a) 4-level type 1 (b) 4-level type 2

Fig. 18. 4-level converter for high speed drive.

The 4-level converter has an additional charge capacitor *C2*, a power switch *QB* and a diode *DF* compared with general asymmetric one. In the type 2, the power diode D_F is included as an anti-parallel diode of power switch Q_B. So, it can reduce the additional power devices to implement the 4-level converter. The charge capacitor C_2 recovers energy from the phase during demagnetization, and the phase current is quickly reduced due to the high negative bias. Then the charged high voltage is through the power switch Q_B to the next excitation phase winding for the fast phase current build-up in type 1. Differ from the type 1, the power switch of the type 2 is controlled to keep the boost voltage as a fixed value. And the excitation voltage is same as the conventional asymmetric converter.

Fig. 19, 20 and 21 show the operating modes of the 4-level type 1 and 4-level type 2. In the fast excitation mode(Fig. 19(a)), dc-link voltage V_{dc} and charged voltage V_{cd} are supplied to excite the phase winding, then the excited phase current builds up fast by the high positive voltage. Similarly, the demagnetized phase current during turn-off is decreased quickly by the high negative bias in the fast demagnetization mode(Fig. 19(d) and Fig. 20(d)). The excitation and wheeling modes are same as the conventional asymmetric converter. However, the demagnetization mode(Fig. 20(c)) supplies the negative boost voltage to the phase current.

The 4-level type 1 is very useful to the high speed drive due to the fast excitation and fast demagnetization modes. However, the boost voltage which is charged in C_2 should be controlled to keep the constant value. To prevent the higher charged voltage, the boost voltage is always adjusted, so the additional voltage sensor is required. In order to discharge the higher boost voltage, the fast excitation voltage can be supply in the positive torque region. So, the control scheme is very complex. Compare with type 1, the boost voltage of the type 2 is automatically adjusted by the gate resistor R_{m1} and R_{m2}. And the operating modes are always independent. This makes easy control of the SRM. And it can reduce the power devices to implement 4-level, although fast excitation is impossible. But, it supplies negative boost voltage during the demagnetization mode, and the current control is easier than the type 1.

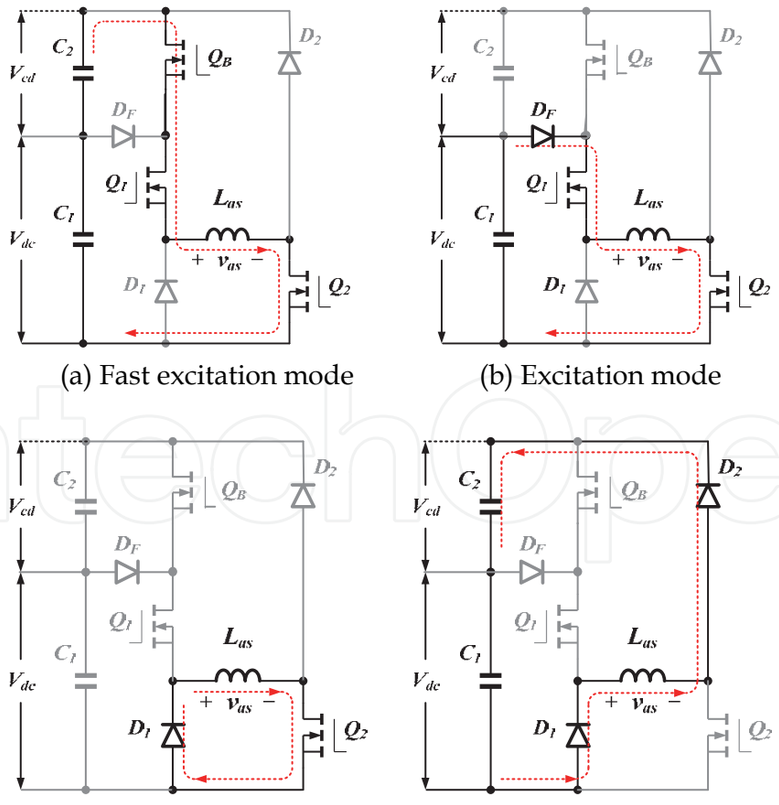

(a) Fast excitation mode (b) Excitation mode

(c) Wheeling mode (d) Fast demagnetization mode

Fig. 19. Operating modes of the 4-level converter (type 1).

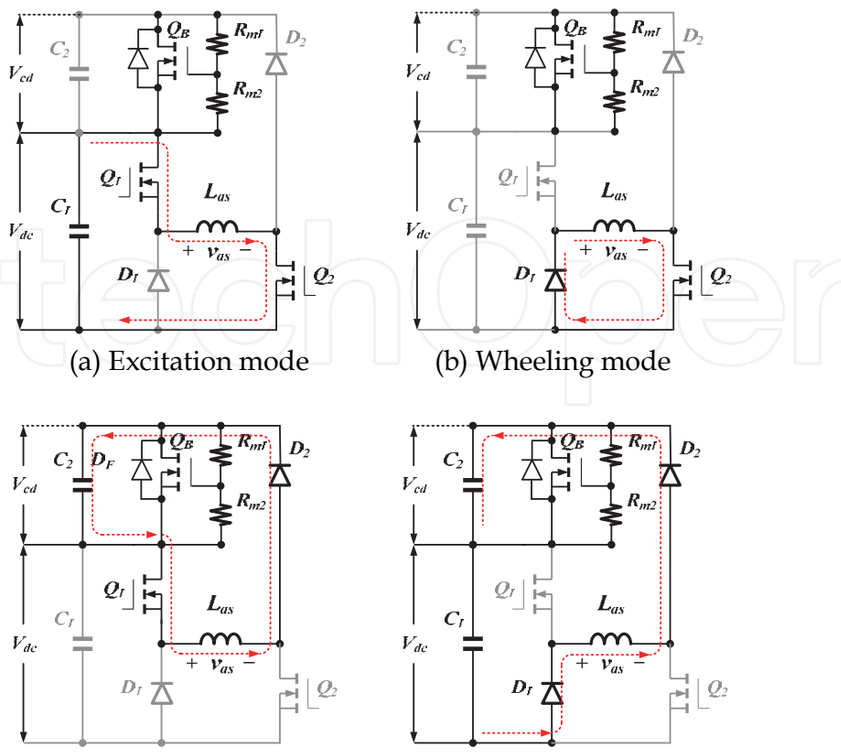

(a) Excitation mode (b) Wheeling mode

(c) Demagnetization mode (d) Fast demagnetization mode

Fig. 20. Operating modes of the 4-level converter (type 2).

With a PWM(Pulse Width Modulation) technology, two operating modes can be used in a sample time to control the phase current.

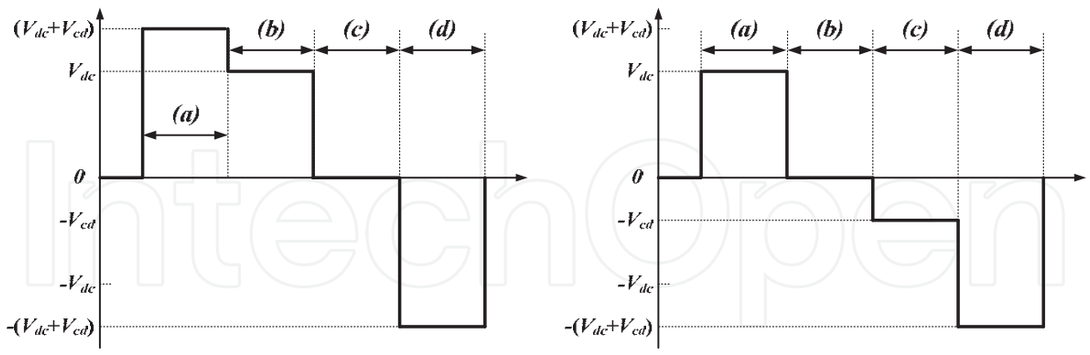

(a) Phase voltage of the type 1 (b) Phase voltage of the type 2

Fig. 21. Phase voltage of the 4-level converter.

Fig. 22 shows current waveform of the 4-levle converter type 1 and asymmetric one at 10,000[rpm] from experiment in a 12/8 SRM. As shown in Fig. 22, excitation current of the 4-level converter can support fast build-up and commutation of phase current when compared with a conventional asymmetric converter. Another approach using 4-level converter is DITC method. In the torque control, the additional control mode is very effective.

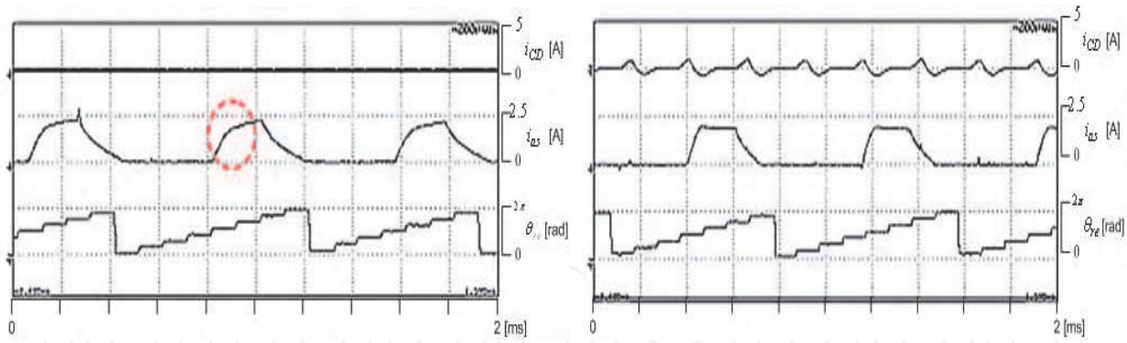

(a) Asymmetric converter (b) 4-level converter type 1

Fig. 22. Comparison of current waveform(10,000[rpm]).

Fig. 23 shows the proto-type high speed 4/2 SRM. The outer radius of the rotor is not constant to produce a wide and a constant positive torque. From this, it has asymmetric inductance which is wide positive and a short negative torque region.

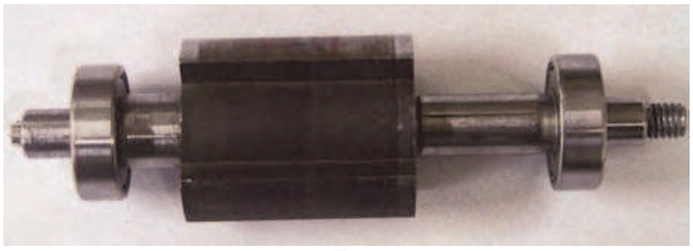

(a) Rotor

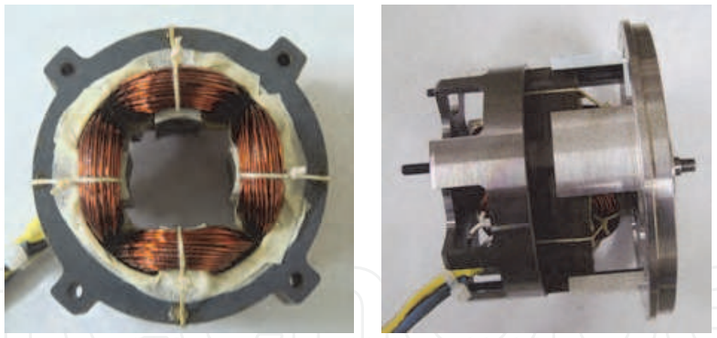

(b) Stator (c) Assembled SRM

Fig. 23. Proto-type high speed 4/2 SRM.

Fig. 24 and 25 show the simulation results of the 4-level type 2. The proto-type motor is 4/2 SRM which has asymmetric inductance. The proto-type SRM has wide positive torque region with over-lap between the phases, and designed for unidirectional applications.
Fig. 24 shows the compared simulation results with conventional asymmetric converter and the proposed 4-level type 2 at 30,000[rpm] with rated load 0.2[Nm] in the proto-type motor. As shown in Fig. 24, the tail current which is extended to the negative torque region produces an additional torque ripple. Compared with Fig. 24(a), the proposed control scheme shown in Fig. 24(b) can reduce the tail current and torque ripple due to the fast demagnetization with a high negative voltage level.

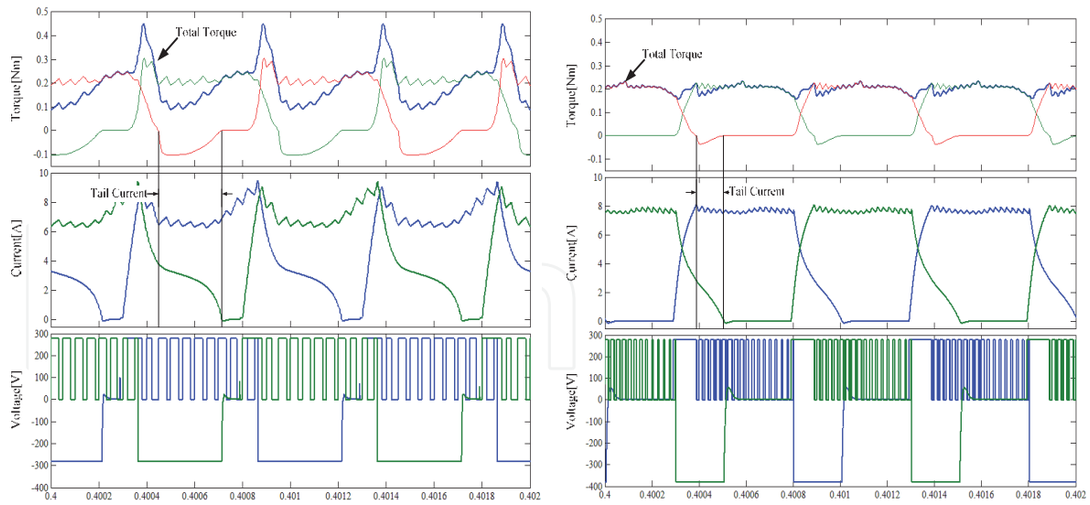

(a) Asymmetric converter (b) 4-level converter type 2

Fig. 24. Compared simulation results(30,000[rpm]).

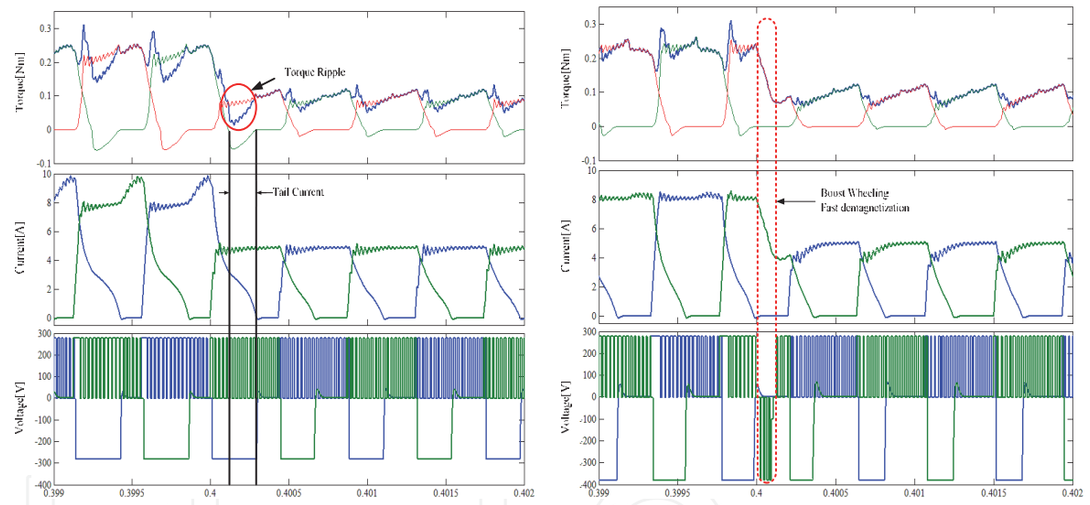

(a) Asymmetric converter (b) 4-level converter type 2

Fig. 25. Compared simulation results with reference variation.

When the reference current is sudden changed, an additional boost wheeling and fast demagnetization mode of the proposed 4-level type 2 can reduce the torque ripple and enhance the control dynamics shown in Fig. 25. Compare to Fig. 25(a), the proposed control scheme (Fig. 25(b)) shows less torque ripple next to the variation point as result of the boost wheeling and fast demagnetization.

4.2 Negative torque compensation

Another approach in the torque control for the high speed SRM, is torque compensation method. Fig. 26 shows the TSF algorithm in the general speed and the high speed region. As shown in Fig. 26(a) and Fig. 26(b), the each torque references are changed to the current reference to produce the reference torque with the considerations of non-linear torque

characteristics. The controlled current can keep the reference torque in the conventional speed region shown in Fig. 26(a). However, the practical current cannot be kept the reference value due to the short commutation time in the high speed region. So, the tail current which is extended to the negative torque region, produces negative torque when the phase is inactive. From this tail current, the total torque of the high speed SRM has high torque ripple shown in Fig. 26(b).

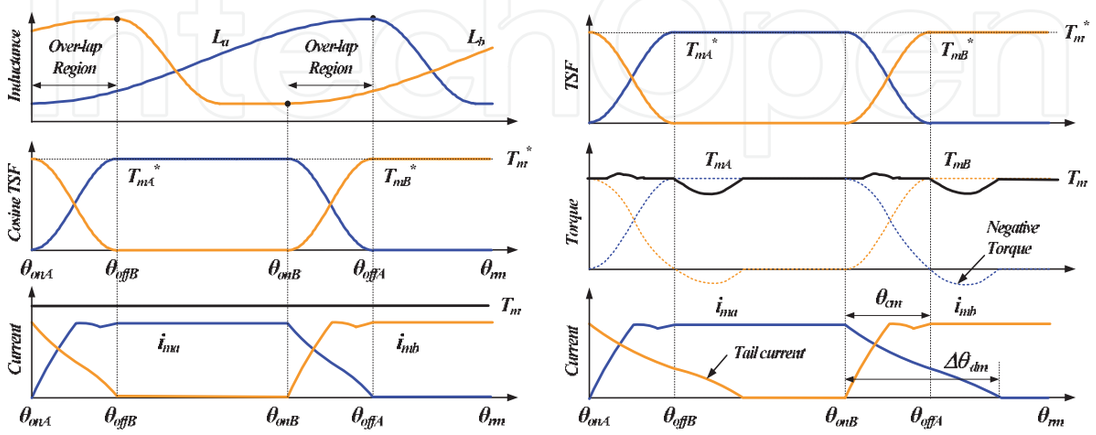

(a) Conventional speed region (b) High speed region

Fig. 26. Torque and current in TSF according to the speed.

In order to compensate the torque ripple from the tail current, the modified TSF control scheme is proposed. The proposed TSF has compensating torque block in the active phase. And the compensating torque can reduce the torque ripple from the negative torque of the inactive phase in a high speed. In order to reduce the tail current during commutation region, the switching signal of the outgoing phase is fully turned off. If the phase current is not extended to the negative torque region, the switching patterns of the each phases are determined by the torque errors during commutation region. However, the swtching signals of the outgoing phase are fully turned off, when the demagentization time is over than the designed commutation angle to reduce the negative torque from the tail current. And the torque error of the outgoing phase is compensated by the incoming phase current reference. After the commutation region, the negative torque of the outgoing phase is compensated by the compensation torque of the active phase.

Fig. 27 shows the block diagram of the proposed TSF control scheme for a high speed region. Compared with the conventional TSF method shown in Fig. 27(b), it has torque compensators and PWM limit signals.

In the Fig. 27, T_{cA}^* and T_{cB}^* are the compensating torques for the negative torques from the tail current. The compensating torque is simply calculated without any control gains as follows.

$$\begin{aligned} T_{cA}^* &= T_{mB}^* - T_{mb} \\ T_{cB}^* &= T_{mA}^* - T_{ma} \end{aligned} \tag{11}$$

Where, $T_{mA}^*$and T_{mB}^* are torque references of the each phases. And the T_{mA} and T_{mB} are the estimated torques which are calculated by the look-up table according to the actual phase

current and rotor position. The EN_A and EN_B are the enable signals for the compensation controller.

The Current Reference block in Fig. 27(b) is designed as look-up table whose data are defined by the reference torque and rotor position with the non-linear characteristics of the proto-type SRM. Fig. 28 shows the torque estimator and current reference data which are used in this paper. The current controller is designed by the PI controller.

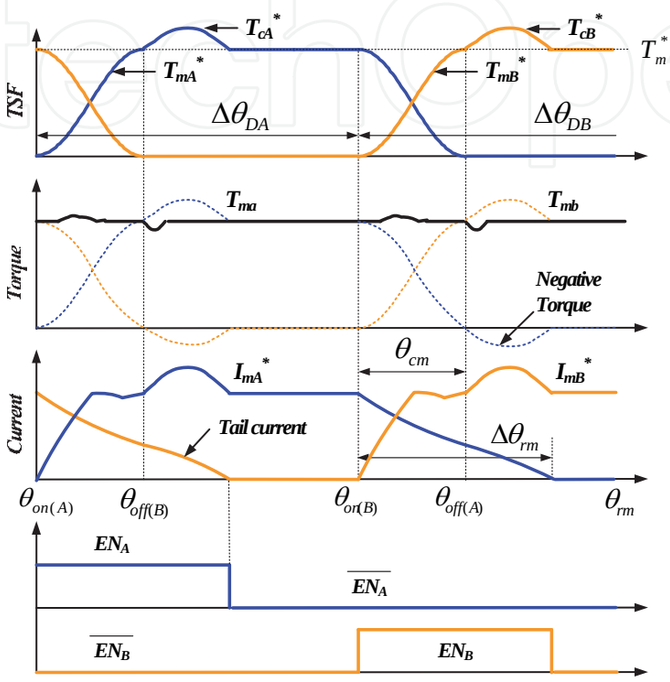

(a) Modified torque sharing function

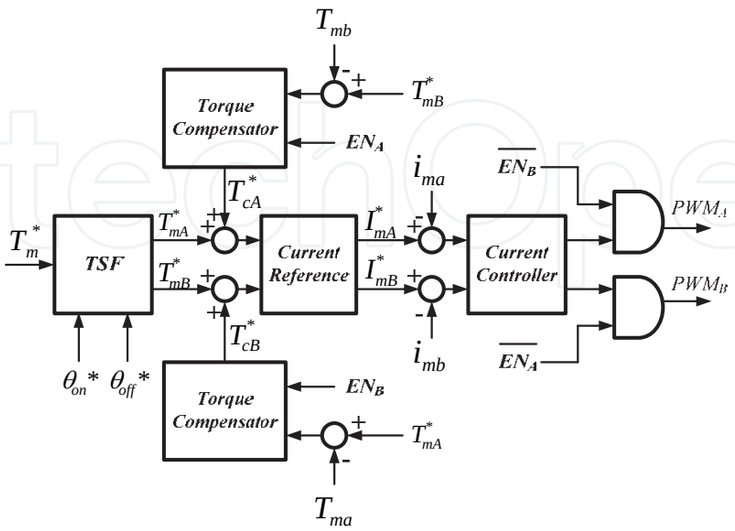

(b) Control block diagram

Fig. 27. Proposed modified TSF control scheme.

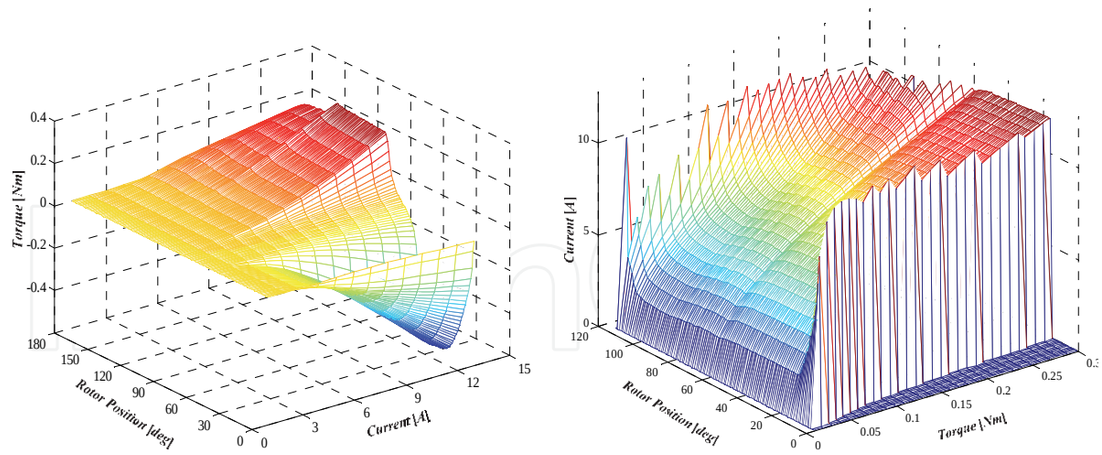

(a) Look-up table of the torque estimator (b) Look-up table of the current reference

Fig. 28. The torque estimator and current reference of the proto-type SRM.

Fig. 29 shows the compared simulation results in the conventional TSF and the proposed control scheme at 10,000[rpm]. As shown in Fig. 29, the simulation results of the proposed type are marginally improved, and the torque ripple is almost same due to the a small tail current. In the 10,000[rpm], the negative torque is very small and the compensation effect is not much. The output torque of the high speed SRM can be controlled well by the TSF control scheme.

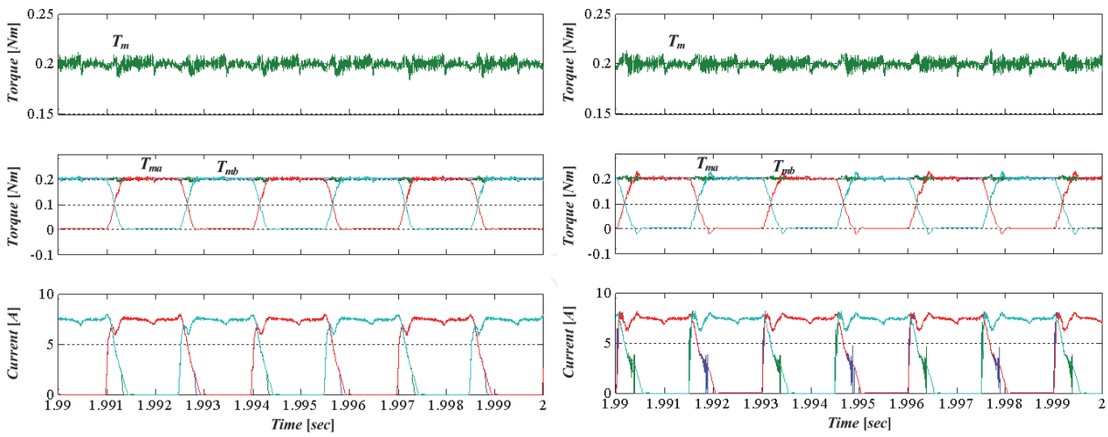

(a) Conventional cosine TSF (b) Proposed TSF control scheme

Fig. 29. Compared simulation result at 10,000[rpm].

Fig. 30 shows the compared simulation results at 30,000[rpm]. As shown in Fig. 30, the torque ripple of the proposed control scheme is much reduced than the conventional one. The torque ripple of the conventional TSF is very serious after the commutation region due to the negative torque from the tail current of the outgoing phase winding. However, the proposed control scheme can compensate the negative torque with the active phase torque.

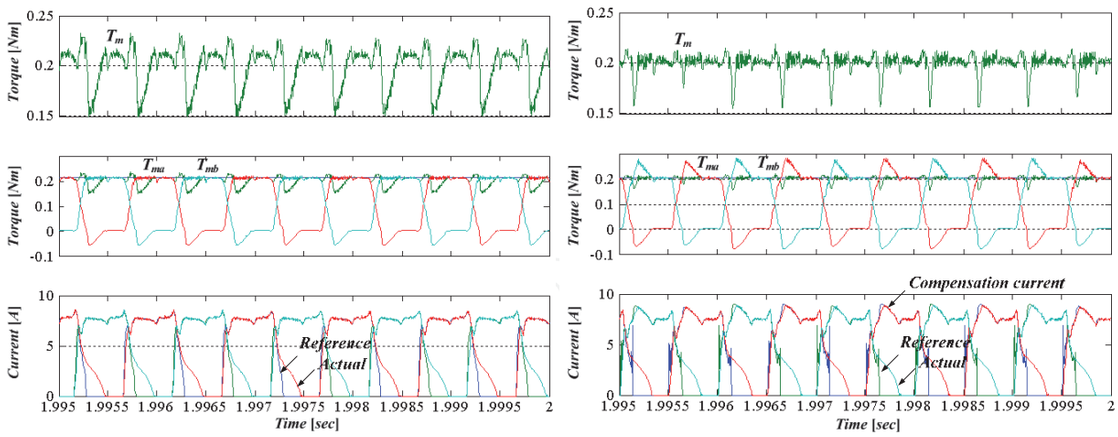

(a) Conventional cosine TSF (b) Proposed TSF control scheme

Fig. 30. Compared simulation result at 30,000[rpm].

Fig. 31 shows the compared experimental results according to the control schemes at 10,000[rpm] and no-load. With the conventional cosine TSF shown in Fig. 31(a), phase current can compensate the non-linear torque and constant torque can be achieved. In the proposed control scheme, the torque control performance is similar to the conventional cosine TSF. It is because that the outgoing phase current can be exhausted during the commutation region in the low speed and no load.

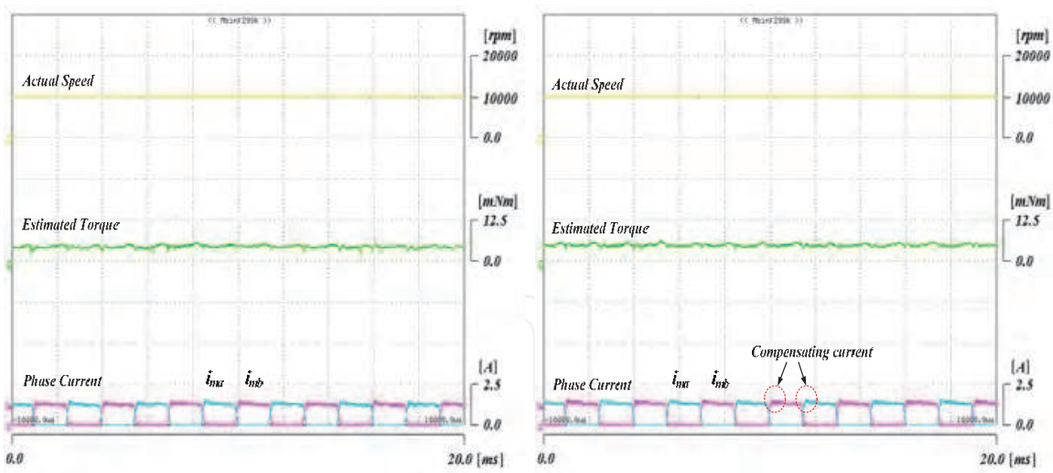

(a) Conventional cosine TSF (b) Proposed TSF control scheme

Fig. 31. Compared experimental results (At 10,000[rpm]).

Fig. 32 shows the experimental results at 30,000[rpm]. As shown in Fig. 32, the current of outgoing phase is not exhausted in the commutation region. And the tail current produces torque ripple as shown in Fig. 32(a). In the proposed control scheme, the incoming phase current can compensate the negative torque from tail current, and the torque ripple can be much decreased as shown in Fig. 32(b).

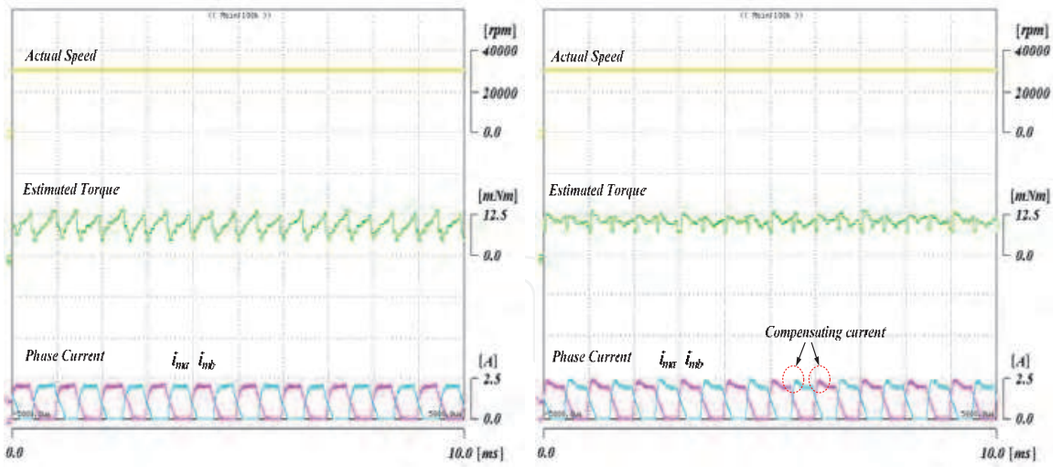

(a) Conventional cosine TSF (c) Proposed TSF control scheme

Fig. 32. Compared experimental results (At 30,000[rpm]).

Fig. 33 shows the experimental results with a practical heavy load fan. The fan load is increased according to the speed. In the 10,000[rpm], the tail current which is extended to the negative torque region produces high torque ripple as shown in Fig. 33(a). The compensation current can suppress the negative torque as shown in Fig. 33(b).

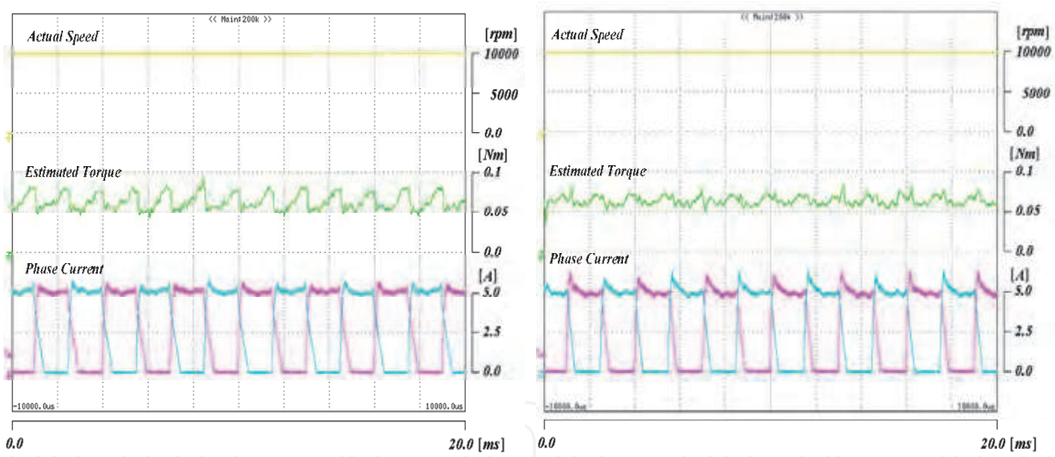

(a) Conventional cosine TSF (b) Proposed TSF control scheme

Fig. 33. Experimental results of heavy fan load (At 10,000[rpm]).

5. Conclusion

The reasons of the torque ripple in SRM are the inherent torque dead-zone from the design scheme, non-linear torque characteristics and the negative torque in a high speed region.
The inherent torque dead-zone can be removed by the design approach in two-phase SRM and Hybrid single-phase SRM. This torque ripple source cannot be removed by the control approach due to the inherent torque production mechanism of SRM.
Various torque control approaches can reduce the torque ripple from the non-linear torque characteristics of SRM. DTC and TSF method are good choice to improve the torque control

performance although they require a complex torque data of the practical motor. However, the performance of the current controller is much decreased. So, the conventional torque control scheme has torque ripple due to the current error and tail current. In order to reduce the tail current and current error in a high speed region, advance converter topologies which can supply additional boost voltage to increase the current control performance are introduced. These converters can reduce the current error in the torque control scheme, and it can improve the torque control performance in the high speed region. The negative torque from the tail current during the high speed can be compensated by the simple compensation technology. The detailed control scheme to compensate the negative torque is presented. The simulation and experimental results show the effectiveness the advanced converter topologies and torque compensation technology.

6. Acknowledgment

This work was supported by Energy Resource R&D program (2009T100100654) under the Ministry of Knowledge Economy, Republic of Korea.

7. References

A. K. Jain, N. Mohan, "SRM power converter for operation with high demagnetization voltage", Industry Applications, IEEE Transactions on, vol. 41, Issue 5, pp.1224-1231, Sept.-Oct. 2005.

A. Dahmane, F. Meebody, F.-M. Sargos, "A novel boost capacitor circuit to enhance the performance of the switched reluctance motor", Power Electronics Specialists Conference, 2001, pp.844-849, 17-21 Jun. 2001.

B.H. Bae, S. K. Sul, J.H. Kwon, J.S. Shin, "Implementation of sensorless vector control for super-high speed PMSM of turbo-compressor", in Proc. IEEE Industry Applications Conf., vol.2, Oct. 2001, pp.1203–1209.

C. H. Choi, S. H. Kim, Y. D. Kim, and K.H. Park, "A new torque control method of a switched reluctance motor using a torque-sharing function," IEEE Trans. on Magnetics, vol. 38, no. 5, September 2002, pp. 3288-3290.

C. Sreekumar, V. Agarwal, "A Hybrid Control Algorithm for Voltage Regulation in DC–DC Boost Converter," IEEE Trans. on Industrial Electronics, vol. 55, no. 6, pp. 2530-2538, June 2008.

D.H. Lee, J. Liang, Z.G. Lee, and J. W. Ahn," A Simple Nonlinear Logical Torque Sharing Function for Low Torque Ripple SR Drive", Industrial Electronics, IEEE Transactions on, vol. 56, no.8, pp. 3021-3028, 2009.

D. H. Lee, J. W. Ahn, "A Novel Four-Level Converter and Instantaneous Switching Angle Detector for High Speed SRM Drive", IEEE Trans. on Power Elctronics, Vol. 22, No. 5, pp. 2034-2041, 2007.

D. H. Lee, J. W. Ahn, "Design and Analysis of Hybrid Stator Bearingless SRM", Journal of Electrical Engineering & Technology, Vol. 5, No. 4, pp. 571-579, Sep. 2010.

D. H. Lee, Lee Zhen-Guo, Liang Jianing, Ahn Jin-Woo, "Single-Phase SRM Drive With Torque Ripple Reduction and Power Factor Correction", IEEE Trans. on Industry Applications, Vol 43, Issue 6, Nov.-dec. 2007 pp.1578 - 1587

D. S. Schramm, B. W. Williams, and T. C. Green, "Torque ripple reduction of switched reluctance motors by phase current optimal profiling," in Proc. IEEE-PESC Conf. Rec.'92, 29 June-3 July 1992, pp. 857-860.

E. E. Kharashi, "Design and Analysis of Rolled Rotor Switched Reluctance Motor", Journal of Electrical Engineering and Technology, vol. 1, no. 4, pp. 472-481, 2006.

G. Dessouky, B. W. Williams, and J. E. Fletcher, "A novel power converter with voltage boosting capacitors for a four-phase SRM drive," IEEE Trans. Ind. Electron., vol. 45, no. 5, pp. 815-823, Oct. 1998.

H. Hannoun, M. Hilairet, C. Marchand, "Design of an SRM Speed Control Strategy for a Wide Range of Operating Speeds", IEEE Trans. on Industrial Electronics, Vol. 57, No. 9. Pp. 2911-2921, 2010.

I. Husain, "Minimization of torque ripple in SRM drives," IEEE Trans. on Industrial Electronics, vol. 49, no. 1, Feb. 2002, pp. 28-39.

I. Husain, M. Ehsani, "Torque ripple minimization in switched reluctance motor drives by PWM current control", IEEE Trans. on Power Electronics, vol. 11, no. 1, January 1996, pp. 83-88.

I.R. Kartono, K. Kajiwara, H. Dohmeki, "Dynamic simulation of maximizing the starting torque for super-high-speed drive of a 4/2 Switched Reluctance Motor", IEEE International Conference of Electrical Machines and System, pp.1-6, Sept. 2008.

J. C. Moreira, "Torque ripple minimization in switched reluctance motors via bi-cubic spline interpolation," in Proc. IEEE-PESC Conf. Rec.'92, 29 June-3 July 1992, pp. 851-856.

J. D. Lewis, H. R. Bolton, and N. W. Phillips, "Performance enhancement of single and two phase SR drives using a capacitor boost circuit," in European Power Electronics and Applications Conf. Rec., vol. 3, pp. 229–232, 1995.

J. F. Pan, N. C. Cheung, W. C. Gan, S. W. Zhao, "A Novel planar switched reluctance motor for industrial applications", IEEE Trans. on Magnetics, vol. 42, no. 10, Oct. 2006, pp.2836 – 2839.

J. Liang, D.H. Lee, J.W. Ahn, "A novel 4-level converter and instantaneous switching angle detector for high speed SR drive", in Proc. IEEE Power Electronics Specialists Conf. Jun. 2006, pp.1478~1483.

J. Liang, D. H. Lee, and J. W. Ahn, "Direct instantaneous torque control of switched reluctance machines using 4-level converters", Electric Power Applications, IET Transactions on, vol. 3, Issue 4, pp.313-323, Jul. 2009.

J. W. Ahn, S. J. Park, and D. H. Lee, "Hybrid excitation of SRM for reduction of vibration and acoustic noise," IEEE Trans. on Industrial Electronics, vol. 51, no. 2, April 2004, pp. 374-380.

J. W. Ahn, Sung-Jun Park, Dong-Hee Lee, "Novel encoder for switching angle control of SRM", IEEE Trans. on Industrial Electronics, vol. 53, no. 3, June 2006, pp. 848-853.

J. W. Ahn, T. H. Kim, D. H. Lee, "Performances of SRM for LSEV," Journal of Power Electronics, vol.5, no.1, Jan. 2005, pp. 45-54.

Kouta Kajiwara, Yong-Jae Kim, Hideo Dohmeki, "Analysis of the maximizing start torque of Switched Reluctance Motor for super high speed drive", Electrical Machines and Systems, ICEMS, pp.1428-1432 , Oct. 2007.

K. I. Hwu, C. M. Liaw, " DC-link voltage boosting and switching control for switched reluctance motor drives", Electric Power Applications, vol. 147, Issue 5, pp. 337-344, Sept. 2000.

K. Ohyama, M. Naguib, F. Nashed, K. Aso, H. Fujii, H. Uehara, "Design using finite element analysis of a switched reluctance motor for electric vehicle," Journal of Power Electronics, vol.6, no.2, April 2006, pp. 163-171.

K. Xin, Q. Zhan, J. Luo, "A new simple sensorless control method for switched reluctance motor drives", Journal of Electrical Engineering & Technology, vol. 1, no. 1, March, 2006. pp. 52-57.

L. Xu, C. Wang, "Accurate Rotor Position Detection and Sensorless Control of SRM for super-high Operation", IEEE Trans. on Power Electronics, Vol. 17, No. 5, pp. 757-763, 2002.

M. Dahmane, F.M. Tabar, F.M. Sargos, "An adapted converter for switched reluctance motor/generator for high speed applications", in Record, IEEE Industry Applications Conf. vol. 3, Oct. 2000, pp.1547-1554.

M. N. F. Nashed, K. Ohyama, K. Aso, H. Fujii, H. Uehara, "Automatic Turn-off Angle control for High Speed SRM Drives", Journal of Power Electronics, vol. 2, no. 1, pp. 81-88, 2007.

M. Krishnamurthy, C. S. Edrington, A. Emadi, P. Asadi, M. Ehsani, B. Fahimi, "Making the case for applications of switched reluctance motor technology in automotive products", IEEE Trans. on Power Electronics, vol. 21, no. 3, May 2006, pp. 659-675.

M.A. Rahman, A. Chiba, T. Fukao, "Super high speed electrical machines-summary", in Proc. Power Engineering Society General Meeting IEEE 6-10, vol.2, Jun. 2004, pp. 1272–1275.

N. Bianchi, S. Bolognani, F. Luise, "High speed drive using a slotless PM motor", IEEE Transactions on Power Electronics, vol.21, no.4, pp. 1083- 1090, July 2006.

R. C. Kavanagh, J. M. D. Murphy, and M. G. Egan, "Torque ripple minimization in switched reluctance drives using self-learning techniques," in Proc. IEEE-IECON Conf. Rec.'91, 28 Oct.-1 Nov. 1991, pp. 289-294.

R. Krishnan, Switched Reluctance Motor Drives: Modeling, Simulation, Analysis, Design, and Applications, CRC Press, 2001

R. Krishnan, D. Blanding, A. Bhanot, A. M. Staley, N. S. Lobo, "High reliability SRM drive system for aerospace applications.", in Proc. Industrial Electronics Society(IECON '03), vol. 2, Nov. 2003, pp. 1110-1115.

S. A. Bortoff, R. R. Kohan, R. Milman, "Adaptive Control of Variable Reluctance Motors : a Spline Function Approach", IEEE Trans. on Industrial Electronics, Vol. 45, No. 3, pp. 433-444, 1998.

S. Chan, H. R. Bolton, "Performance enhancement of single-phase switched-reluctance motor by DC link voltage boosting", Electric Power Applications, IEE Proceedings, Issue 5, Vol.2, pp.316-322, Sept. 1993

S. H. Won, J. H. Choi, J. Lee, “Windage Loss Reduction of High-Speed SRM Using Rotor Magnetic Saturation”, IEEE Trans. on Magnetics, Vol. 44, No. 11, pp. 4147-4150, 2008.

S. I. Nabeta, I. E. Chabu, L. Lebensztajn, D. A. P. Correa, W. M. da Silva, ; K. Hameyer, "Mitigation of the Torque Ripple of a Switched Reluctance Motor Through a Multiobjective Optimization", IEEE Transactions on Magnetics, Vol. 44, Issue 6, June 2008, pp.1018 – 1021

S. Kozuka, N. Tanabe, J. Asama, A. Chiba, "Basic characteristics of 150,000r/min switched reluctance motor drive", Power and Energy Society General Meeting - Conversion and Delivery of Electrical Energy in the 21st Century, pp.1-4, July 2008.

S. K. Mondal, S. N. Bhadra, S. N. Saxena, “Application of current-source converter for use of SRM drive in transportation area” in Proc. Power Electronics and Drive Systems Conf., vol. 2, May 1997, pp.708-713.

S. M. Lukic, A. Emadi, “State-Switching Control Technique for Switched Reluctance Motor Drives : Theory and Implementation”, IEEE Trans. on Industrial Electronics, Vol. 57, No. 9, pp. 2932-2938, 2010.

S. Mir, I. Husain, and M. E. Elbuluk, “Energy-efficient c-dump converters for switched reluctance motors,” IEEE Trans. Power Electron., vol. 12, no. 5, pp. 912–921, Sep. 1997.

T. Raminosoa, B. Blunier, D. Fodorean, A. Miraoui, “Design and Optimization of a Switched Reluctance Motor Driving a Compressor for a PEM Fuel-Cell System for Automotive Applications”, IEEE Trans. on Industrial Electronics, Vol. 57, No. 9, pp. 2988-2997, 2010.

T. Genda, H. Dohmeki, "Characteristics of 4/2 Switched Reluctance Motor for a high speed drive by the excitation angle", International Conference on Electrical Machines and Systems, ICEMS 15-18, pp.1-6, Nov 2009.

V. P. Vujicic, S. N. Vukosavic, M. B. Jovanovic, “Asymmetrical switched reluctance motor for a wide constant power range”, IEEE Trans. on Energy Conversion, vol. 21, no. 1, Mar. 2006, pp.44-51.

W.L. Soong, G.B. Kliman, R. N. Johnson, R.A. White, . J.E. Miller, “Novel high speed induction motor for a commercial centrifugal compressor”, in Proc. IEEE IAS Annual Meeting, vol.1, Oct. 1999, pp. 494-501.

X. D. Xue, K. W. E. Cheng, N. C. Cheung, “Multi-Objective Optimization Design of In-Wheel Switched Reluctance Motors in Electric Vehicles”, IEEE Trans. on Industrial Electronics, Vol. 57, No. 9, pp. 2980-2987, 2010.

Y. H. Yoon, Y. C. Kim, S. H. Song, C. Y. Won, “Control of C-dump Converters fed from Switched Reluctance Motors on an Automotive Application,” Journal of Power Electronics, vol.5, no.2, April 2005, pp. 120-128.

Y. K. Choi, H. S. Yoon, C. S. Koh, "Pole-Shape Optimization of a Switched-Reluctance Motor for Torque Ripple Reduction", IEEE Trans. on Magnetics, Vol. 43, Issue 4, April 2007, pp.1797 - 1800

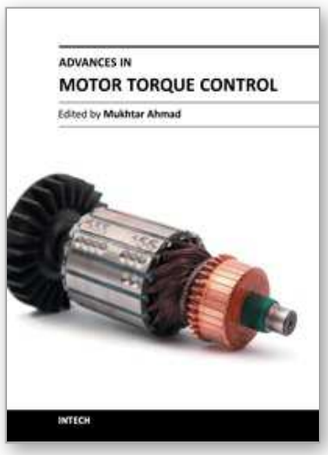

Advances in Motor Torque Control

Edited by Dr. Mukhtar Ahmad

ISBN 978-953-307-686-7
Hard cover, 144 pages
Publisher InTech
Published online 22, September, 2011
Published in print edition September, 2011

Electric motors are widely used in industries to convert electrical energy into mechanical form. Control techniques are designed to improve the performance and efficiency of the drive so that large amounts of electrical energy can be saved. This book is primarily written with the objective of providing necessary information on use of electric motors for various applications in industries. During the last ten years a number of methods of control of electric drives have emerged. Some of these methods are described in this book. The reader will be able to understand the new methods of control used in drives, e.g. direct and sensorless control. Also the application of motor control in dentistry, the effect of human reaction and improvement of the efficiency of drives with control have been described.

InTech Europe
University Campus STeP Ri
Slavka Krautzeka 83/A
51000 Rijeka, Croatia
Phone: +385 (51) 770 447
Fax: +385 (51) 686 166
www.intechopen.com

InTech China
Unit 405, Office Block, Hotel Equatorial Shanghai
No.65, Yan An Road (West), Shanghai, 200040, China
中国上海市延安西路65号上海国际贵都大饭店办公楼405单元
Phone: +86-21-62489820
Fax: +86-21-62489821

IntechOpen